

# H6-type transformerless single-phase inverter for grid-tied photovoltaic system

ISSN 1755-4535  
Received on 20th April 2014  
Accepted on 7th October 2014  
doi: 10.1049/iet-pel.2014.0251  
www.ietdl.org

Monirul Islam, Saad Mekhilef ✉

Power Electronics and Renewable Energy Research Laboratory (PEARL), Department of Electrical Engineering, University of Malaya, Kuala Lumpur 50603, Malaysia  
✉ E-mail: saad@um.edu.my

**Abstract:** There has been an increasing interest in transformerless inverter for grid-tied photovoltaic (PV) system because of the benefits of lower cost, smaller volume as well as higher efficiency compared with the ones with transformer. However, one of the technical challenges of the transformerless inverter is the safety issue of leakage current which needs to be addressed carefully. In addition, according to the international regulations, transformerless inverter should be capable of handling a certain amount of reactive power. In this study, a new H6-type transformerless inverter for grid-tied PV system is proposed that can eliminate the threat of leakage current. The proposed topology has also the capability to inject reactive power into the utility grid. Three-level output voltage employing unipolar sinusoidal pulse-width modulation can be achieved with the proposed topology. The proposed topology structure and detail operation principle with reactive power control are investigated. The relationship among the existing topologies and their reactive power control capability are also discussed. The proposed topology is simulated in MATLAB/Simulink software to initially verify the accuracy of theoretical explanations. Finally, a universal prototype rated 1 kW has been built and tested. The experimental results validate the theoretical analysis and simulation results.

## 1 Introduction

Renewable energy technologies are becoming less expensive and more efficient, which have made it an attractive solution of recent energy crises [1, 2]. Furthermore, renewable energy sources have the advantage that the power is produced in close proximity to where it is consumed. This way the losses because of transmission lines are not present. Among a variety of renewable energy sources, photovoltaic (PV) is predicted to have biggest generation, up to 60% of the total energy by the end of this century [3, 4], because the energy which converted into electrical energy, is the light from the sun is free, available almost everywhere and will still be present for millions of years long after all non-renewable energy sources have been depleted [3, 5].

The PV generates direct voltage; thus, it requires a converter to convert into a voltage of corresponding amplitude at main frequency for feeding it into utility grid. However, the problem can arise because of the hazardous voltage that can be avoided by providing galvanic isolation between the PV module and the grid through a transformer [6, 7]. Nevertheless, the use of a transformer leads to additional drawbacks such as less efficiency, bulky, more expensive and less durability. In order to overcome these drawbacks, transformerless inverter has been introduced which has the benefits such as lower cost, higher efficiency, smaller size and weight [6, 8]. Owing to the missing galvanic separation, large voltage fluctuation both at main frequency and high frequency that depends on the topology structure and control scheme, resulted in leakage current flow from the PV module to the system through the inevitable parasitic capacitance with respect to ground potential [9, 10]. This ground leakage current increases the grid current harmonics and system losses and also creates a strong conducted and radiated electromagnetic interference [11–13]. Accordingly, some standards have been established to fix a maximum allowable leakage current such as the German DIN VDE 0126-1-1 standard which states that the grid must be disconnected within 0.3 s if the root-mean-square (RMS) value of leakage current is more than 30 mA [14]. The RMS values of the fault or leakage current and their corresponding disconnection times are presented in Table 1.

The half-bridge inverter family can eliminate the difficulties of leakage current and injection of DC current into the utility grid having the necessity of high input voltage (700 V) corresponds to 230 V AC application. On the other hand, the problem of leakage current and high input voltage can be solved by using the bipolar sinusoidal pulse-width modulation (SPWM) full-bridge inverter. However, the conversion efficiency of bipolar SPWM inverter is lower because of the high switching losses and magnetic inductor losses. Therefore to solve the problem of leakage current and low efficiency, many DC–AC inverter topologies based on full-bridge inverter have been proposed [6, 8, 15–25]. Gonzalez *et al.* [8] proposed full-bridge with DC bypass topology, in which two switches and two diodes are added with a full-bridge inverter. It exhibits low leakage current and high efficiency compared with the full-bridge inverter with bipolar modulation. Another topology with DC bypass is proposed in [21], referred as H5 topology. This topology is patented by SMA Solar Technology AG. Schmidt *et al.* [26] proposed a highly efficient and reliable inverter concept (HERIC) topology by adding two extra switches in the AC side of a full-bridge inverter. Two extended HERIC topologies are proposed in [16, 27]. Although these topologies can achieve high efficiency and low leakage current, they have not yet been analysed from the point of view of reactive power handling capacity.

In this study, a new transformerless grid-tied PV inverter topology is proposed based on the conventional full-bridge inverter with two additional power switches, which ensures the DC decoupling at the freewheeling mode. As a result, leakage current is minimised to safe level. The proposed topology is also capable to inject reactive power into utility grid; therefore, it can satisfy the requirement of the standard VDE-AR-N 4105. Finally, to verify the accuracy of theoretical analysis, a prototype inverter rated at 1 kW has been built and tested.

This study is prepared as follows: topology relationship among existing topologies and their reactive power control capability are analysed in Section 2. The proposed circuit structure, detail operation principle with reactive power flow and differential mode (DM) characteristics of the proposed inverter are investigated in Section 3. Simulation and experimental results are depicted in Sections 4 and 5, respectively, and Section 6 concludes the study.

**Table 1** Leakage current value and their corresponding disconnection time described in VDE 0126-1-1 standard [14]

Leakage current value, mA	Disconnection time, s
30	0.3
60	0.15
100	0.04

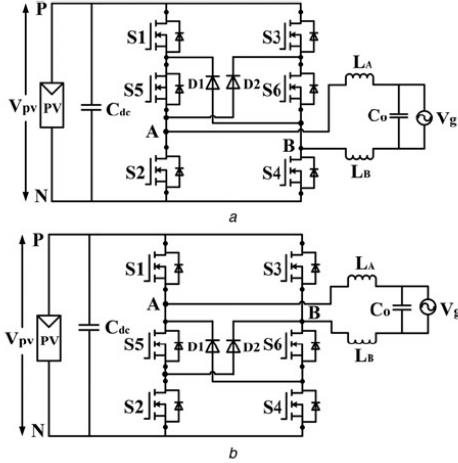


**Fig. 1** Existing H6-type transformerless topologies with almost identical freewheeling path inserted in different position

a H6-I [25]  
b H6-II [19]

## 2 Analysis on existing transformerless topologies

### 2.1 Existing topology relationship analysis

As discussed in the literature, excellent common mode (CM) characteristics can be achieved with the full-bridge topology by

employing bipolar SPWM, but the DM characteristic is poor. In contrast, unipolar SPWM improves the DM characteristics, but the CM characteristic is decreased [25]. Therefore a lot of researches have been conducted on the transformerless PV inverter to achieve an excellent CM and DM characteristics. In Fig. 1, the existing H6-type transformerless topologies (named H6-I and H6-II) which are derived from the conventional H4 topology with almost identical freewheeling path inserted at different position are shown. These topologies are constituted of six metal-oxide-semiconductor field-effect transistor (MOSFET) switches (S1–S6) and two diodes (D1–D2). The operation principle of these topologies is depicted in Figs. 2 and 3. Four operation modes were proposed in each period of the utility grid to generate three-level output voltage state as  $+V_{pv}$ , 0 and  $-V_{pv}$ . It can be seen that the grid current is flowing through three switches which is very similar for both H6-I and H6-II topologies. However, these topologies were proposed to operate with unity power factor (PF) [19, 25]. The CM and DM characteristics of these topologies are presented in Table 2.

According to the above analysis, it can be observed that the CM and DM characteristics and the operation principle of these topologies are almost identical. The only difference among them is the freewheeling branch which is inserted at different position.

### 2.2 Reactive power control capability analysis

Recently, almost every international regulation imposes that a definite amount of reactive power should be handled by the grid-tied PV inverter. This is because of the problem of grid voltage stability. According to the standard VDE-AR-N 4105, grid-tied PV inverter of power rating below 3.68 kVA, should attain PF from 0.95 leading to 0.95 lagging [28]. When the inverter injects or absorbs reactive power, a phase shift is occurred between the voltage and current as shown in Fig. 4. The shifted degree can be calculated as follows

$$\theta = \cos^{-1} \text{PF} \quad (1)$$

where  $\theta$  is the shifted phase and PF is the commanded power factor.

As shown in Fig. 4, the grid voltage and current have opposite polarity in the negative power region. Consequently, the PWM strategy should be changed to draw power in this region. In the

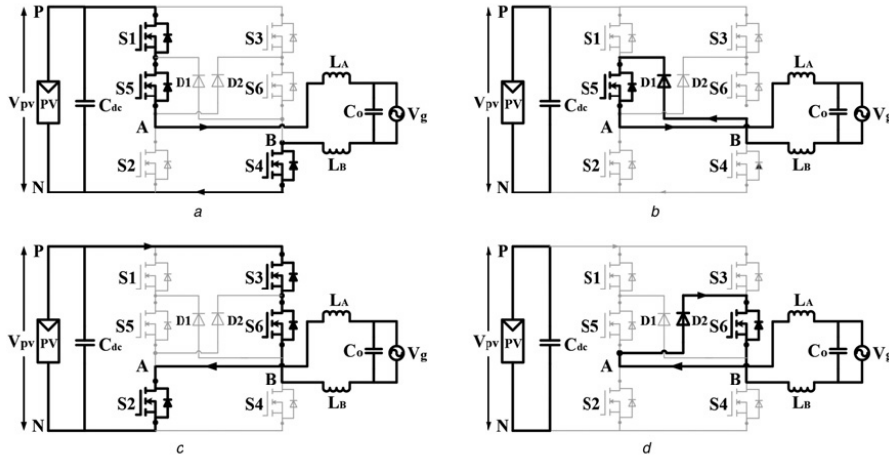


**Fig. 2** Operational modes of H6-I topology [25]

a Active  
b Freewheeling mode in the positive half-cycle of grid current  
c Active  
d Freewheeling mode in the negative half-cycle of grid current

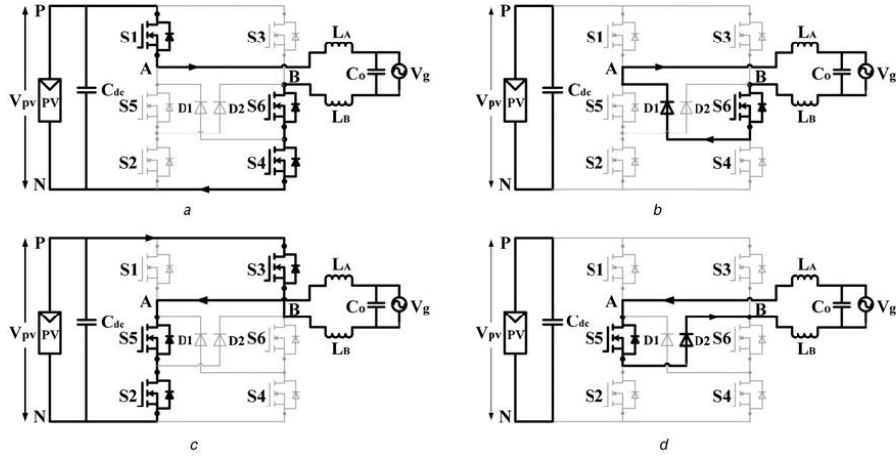


**Fig. 3** Operational modes of H6-II topology [19]  
 a Active  
 b Freewheeling mode in the positive half-cycle of grid current  
 c Active  
 d Freewheeling mode in the negative half-cycle of grid current

case of topologies presented in Fig. 1, the anti-parallel diodes of MOSFETs will be activated if a phase shift is occurred between the voltage and current. Accordingly, the dependability of the system will be reduced because of the MOSFETs anti-parallel diode reverse recovery issues. Therefore the lack of reactive power handling capability constitutes a huge drawback of these topologies.

### 3 Proposed topology and operation principle

#### 3.1 Proposed topology and operation principle

According to the analysis made in Section 2.1, we can derive a new H6-type topology that can overcome the drawback regarding reactive

**Table 2** Comparison of CM and DM characteristics among the topologies shown in Fig. 1 [25]

Hybrid topology	$V_{cm} = (V_{AN} + V_{BN})/2$		$V_{dm} = (V_{AN} - V_{BN})$	
	Level	Frequency	Level	Frequency
H6-I	$V_{pv}/2$	0	$+V_{pv}, 0$ and $-V_{pv}$	$f_s$
H6-II	$V_{pv}/2$	0	$+V_{pv}, 0$ and $-V_{pv}$	$f_s$

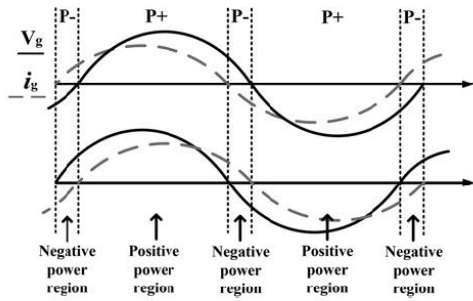


**Fig. 4** Relationship between grid voltage  $V_g$  and current  $i_g$  with leading and lagging PF

power controlling capability. Fig. 5a shows the circuit structure of the proposed H6-type PV inverter topology, where the two diodes are removed and MOSFETs are replaced with insulated-gate bipolar transistors (IGBTs), if compared with the topologies presented in Fig. 1. As a result, some differences are automatically created in the freewheeling path and control signals. An excellent DM and CM characteristics would be possible with the proposed topology by employing unipolar SPWM.

Fig. 5b shows the gate drive signal for the proposed circuit structure. It can be seen that when a phase shift is occurred

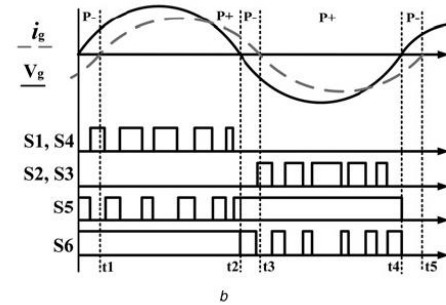
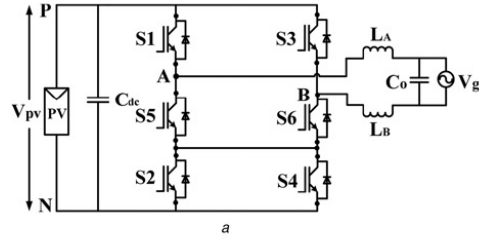


**Fig. 5** Proposed new transformerless grid-tied PV inverter topology  
 a Circuit structure  
 b Control signal

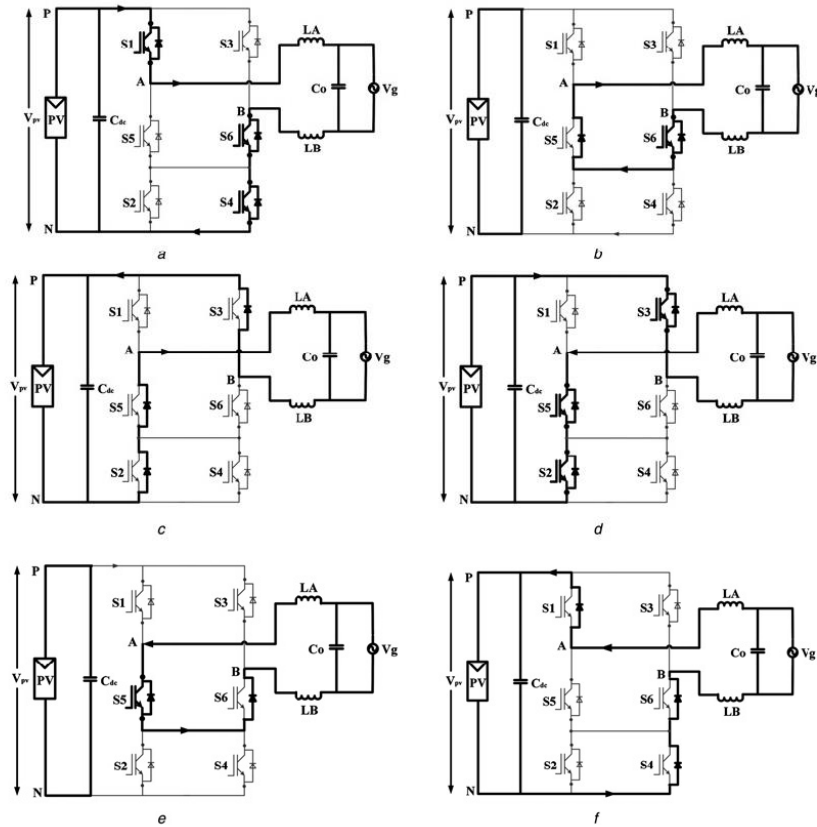


**Fig. 6** Operating principle of the proposed topology with reactive power flow  
*a* Mode 1  
*b* Mode 2  
*c* Mode 3  
*d* Mode 4  
*e* Mode 5  
*f* Mode 6

between the voltage and current, the grid current  $i_g$  remains negative, in the short beginning of positive half period and positive, in the short beginning of negative half period. Therefore the proposed inverter is forced to operate at mode 3 and mode 6 as shown in Fig. 6. However, the proposed inverter operates in four stages within a grid period.

*Stage 1 ( $t1:t2$ ):* This is the positive power region in the positive half-cycle of grid current. In this stage, S6 is always on, whereas S1 and S4 synchronously and S5 complementary commute with switching frequency. Two modes are proposed to generate the output voltage state of  $+V_{PV}$  and 0.

*Mode 1:* This is the active mode in stage 1. This mode starts by turning-on the switches S1 and S4, and the inductor current increases through grid as shown in Fig. 6a. The CM and DM voltages can be defined as follows

$$V_{CM} = \frac{1}{2}(V_{AN} + V_{BN}) = \frac{1}{2}(V_{PV} + 0) = \frac{V_{PV}}{2} \quad (2)$$

$$V_{DM} = (V_{AN} - V_{BN}) = (V_{PV} - 0) = V_{PV} \quad (3)$$

*Mode 2:* This is the freewheeling mode in stage 1. Fig. 6b shows the freewheeling path when S1 and S4 are turned-off. In this mode,  $V_{AN}$  falls and  $V_{BN}$  rises until their values are equal. The inductor current decreases through S6 and the body diode of S5. Therefore  $V_{AN} = V_{PV}/2$  and  $V_{BN} = V_{PV}/2$ . The CM and DM voltages could be calculated in (4) and (5), respectively

$$V_{CM} = \frac{1}{2}(V_{AN} + V_{BN}) = \frac{1}{2}\left(\frac{V_{PV}}{2} + \frac{V_{PV}}{2}\right) = \frac{V_{PV}}{2} \quad (4)$$

$$V_{DM} = (V_{AN} - V_{BN}) = \left(\frac{V_{PV}}{2} - \frac{V_{PV}}{2}\right) = 0 \quad (5)$$

*Stage 2 ( $t2:t3$ ):* This is the negative power region in the positive half-cycle of grid current. In this stage, the inverter output voltage is negative but the current remains positive. In order to generate the output voltage state of  $-V_{PV}$  and 0, the proposed inverter continuously rotates between mode 2 and mode 3, which are shown in Figs. 6b and c. Mode 3 can be explained as follows:

*Mode 3:* In this mode, the switches S2, S3 and S5 are turned-on and the filter inductors are demagnetised. Since the inverter output voltage is negative and the current remains positive, inductor

Link to Full-Text Articles :

<http://digital-library.theiet.org/content/journals/10.1049/iet-pel.2014.0251>